



# An inorganic-organic hybrid supramolecular complex $(\text{H}_3\text{O})_4[(\text{CoC}_{14}\text{H}_{12}\text{N}_2\text{O}_{10})_{1.5}(\text{SiW}_{12}\text{O}_{40})]\cdot 2\text{H}_2\text{O}$ : synthesis, structure, properties, and application to catalytic elimination methanol

Hanxi Xiao, Yuzhe Han, Qian Fang, Qing Cai & Qian Deng

**To cite this article:** Hanxi Xiao, Yuzhe Han, Qian Fang, Qing Cai & Qian Deng (2015) An inorganic-organic hybrid supramolecular complex  $(\text{H}_3\text{O})_4[(\text{CoC}_{14}\text{H}_{12}\text{N}_2\text{O}_{10})_{1.5}(\text{SiW}_{12}\text{O}_{40})]\cdot 2\text{H}_2\text{O}$ : synthesis, structure, properties, and application to catalytic elimination methanol, *Journal of Coordination Chemistry*, 68:15, 2587-2600, DOI: [10.1080/00958972.2015.1064527](https://doi.org/10.1080/00958972.2015.1064527)

**To link to this article:** <http://dx.doi.org/10.1080/00958972.2015.1064527>



Accepted author version posted online: 30 Jun 2015.  
Published online: 21 Jul 2015.



Submit your article to this journal [↗](#)



Article views: 54



View related articles [↗](#)



View Crossmark data [↗](#)

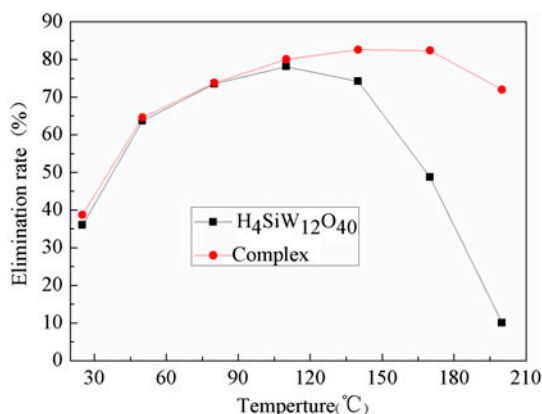
## An inorganic-organic hybrid supramolecular complex $(\text{H}_3\text{O})_4[(\text{CoC}_{14}\text{H}_{12}\text{N}_2\text{O}_{10})_{1.5}(\text{SiW}_{12}\text{O}_{40})] \cdot 2\text{H}_2\text{O}$ : synthesis, structure, properties, and application to catalytic elimination methanol

HANXI XIAO<sup>†</sup>, YUZHE HAN<sup>†</sup>, QIAN FANG<sup>†</sup>, QING CAI<sup>‡</sup> and QIAN DENG<sup>\*†</sup>

<sup>†</sup>Department of Chemistry and Chemical Engineering, Hunan University of Science Technology, Xiangtan, China

<sup>‡</sup>Chemistry Department, City College of New York, City University of New York, New York, USA

(Received 17 February 2015; accepted 4 June 2015)



### Catalytic performance

An organic–inorganic hybrid supramolecular complex,  $(\text{H}_3\text{O})_4[(\text{CoC}_{14}\text{H}_{12}\text{N}_2\text{O}_{10})_{1.5}(\text{SiW}_{12}\text{O}_{40})] \cdot 2\text{H}_2\text{O}$ , is constructed by tungstosilicate anion and 2,3-pyridinedicarboxylic acid cobalt coordination complex via intermolecular forces. Crystal data of the title complex: trigonal system, *P*-3*c*1 space group, *a* = 20.363(3) Å, *b* = 20.363(3) Å, *c* = 27.685(5) Å,  $\alpha = 90^\circ$ ,  $\beta = 90^\circ$ ,  $\gamma = 90^\circ$ , *V* = 9942(3) Å<sup>3</sup>, *Z* = 4, *R*<sub>int</sub> = 0.0383, *R*<sub>2</sub> = 0.1645, GOOF = 1.083. The complex has been hydrothermally synthesized and characterized by Infrared spectra, TG-DTA, fluorescence, cyclic voltammetry, and single-crystal X-ray diffraction. The complex exhibits good catalytic activity for elimination of methanol in the gas phase, when the initial concentration of methanol is 2.76 g m<sup>-3</sup>, and flow rate is 10 mL min<sup>-1</sup> at 140 °C, the elimination rate of methanol is 82.6% over 0.2 g of complex.

**Keywords:** Tungstosilicate acid; Cobalt; Pyridinedicarboxylic acid; Catalytic elimination; Methanol; Organic–inorganic Hybrid

\*Corresponding author. Email: [dengqian10@126.com](mailto:dengqian10@126.com)

## 1. Introduction

Polyoxometalates (POMs) are important building blocks in the construction of functional materials which have properties like multiply charged, multi-morphology, and multi-dimensional adjustable [1]. As “molecular devices”, POMs are a good multi-electron acceptor, which can be used as polydentate ligands. According to the molecular design principles, the metal ions coordinate with ligands to generate organic–inorganic complexes, then combine with polyoxometalates for interesting structures, giving complex structures and properties [2].

Since heteropolyacid chemistry developed, it is cross-promoted and osmosis with solid materials, analysis, organic, physical, biochemical, and energy science; the development of solid inorganic materials have entered a new area.

A variety of layered, chain, porous, and other new nanocluster acid compounds have been synthesized to provide data for heteropolyacid chemistry.

Liu *et al.* [3] have synthesized three complexes with Co, Cu, and Ag, 2,6-pyridine dicarboxylic acid and tungstosilicate. The 2,6-pyridine dicarboxylic acid decomposes in the presence of metal ions for three complexes. Yang *et al.* [4] reported a dilacunary  $\gamma$ -Keggin silicotungstate [ $\gamma$ -SiW<sub>10</sub>O<sub>36</sub>]<sup>8-</sup> by controlling the pH of the reaction system. The two lacunary sites of polyoxoanions are occupied with two [Cu(en)<sub>2</sub>(H<sub>2</sub>O)]<sup>2+</sup> groups via Cu–O–W bonds. A new polyoxometalate complex was hydrothermally synthesized with Cu and 5,6-diamino-1,10-phenanthroline by Yang *et al.* [5]. The complex was used to fabricate a bulk-modified carbon paste electrode (1-CPE). The result indicated that 1-CPE is stable over hundreds of cycles and possessed electrocatalytic activity toward reduction reactions of nitrite.

Felices *et al.* [6] isolated four organic–inorganic hybrid compounds built up of mono lacunary precursor [SiW<sub>11</sub>O<sub>39</sub>]<sup>8-</sup>, copper ion, and 4,4'-bipyridine. Harriman *et al.* [7] reported three Wells-Dawson-type heteropolyanion-supported porphyrin complexes which show excellent photocatalytic activity. By their multiple coordination requirements, electron-rich and unique molecular structures [8], transition metals are suitable to link polyoxometalate building blocks to form new structures with potentially controllable oxophilicity from the molecular level. An unusual antibacterial complex based on polyoxometalate and cobalt-gatifloxacin has been synthesized by Liu *et al.* [9]. The complex has good antibacterial activity and is a low-cost antibacterial compound.

Shen *et al.* [10] synthesized and characterized microtubes of SiMoW<sub>11</sub> Keggin polyoxometalates containing either a Mo(V) or Mo(VI) atom. They found that Mo-substituted Keggin tungstosilicate microtubes in their reduced state are more stable than the all-tungsten Keggin tungstosilicate microtubes. Han *et al.* [11] synthesized a series of all-inorganic, high-nuclearity cobalt-phosphate molecular catalysts. The new compounds are the first POM-based Co–Pi (cobalt–phosphate) cluster molecular catalysts for visible light-driven water oxidation as a functional model of the oxygen-evolving complex in photosystem II (PSII).

Pyridine dicarboxylic acid is a rigid polydentate ligand which has N and O donors. Depending on the location of N and O, heteropolyacid and metal ions could coordinate with pyridine dicarboxylic acid by coordination, H-bonding or  $\pi$ – $\pi$  stacking to form different structures. Therefore, they are valuable building blocks for inorganic–organic complex engineering [12–14].

Due to the interest in these materials, we synthesize an inorganic–organic hybrid complex using 2,3-pyridine dicarboxylic acid, cobalt nitrate, and Keggin-type silicotungstic acid as

reactants by the hydrothermal method. The crystal structure, thermal stability, fluorescence (FL), and oxidation–reduction characteristics of the complex were examined. The catalytic performance for elimination of methanol was explored.

## 2. Experimental

### 2.1. Materials and methods

All chemicals were purchased from commercial sources and used without purification. The crystal structure was determined using a Bruker Smart Apex II CCD area detector single-crystal diffractometer. Infrared spectra (IR) were recorded as KBr pellets on a Perkin-Elmer FTIR-2000 spectrometer. Thermogravimetric differential (TG-DTA) analyses were carried out on a WCT-1-D simultaneous thermal analyzer in air between room temperature and 700 °C at a heating rate of 10 °C min<sup>-1</sup>. UV–vis spectra were measured on a TU-1810 spectrophotometer. Emission/Excitation spectra of FL were obtained on a Hitachi F4500 fluorescence spectrophotometer. Cyclic voltammetry (CV) spectra were tested on an Electrochemical workstation CH1760C of Shanghai Chen-Hua Instrument with the scan rate of 20 mV s<sup>-1</sup>. The products of the catalytic reaction were analyzed online by a GC-9800 gas chromatograph (GC) equipped with a column packed with Porapak-Q and using a flame ionization detector.

### 2.2. Hydrothermal synthesis

Na<sub>2</sub>SiO<sub>3</sub>·9H<sub>2</sub>O (0.0284 g, 0.1 mmol) and Na<sub>2</sub>WO<sub>4</sub>·2H<sub>2</sub>O (0.3597 g, 1.2 mmol) were successively dissolved in 5 mL water, then the pH of the solution was adjusted to 1.75 with 1 : 1 (v : v) H<sub>2</sub>SO<sub>4</sub>. After stirring for 1 h at 60 °C, bright solution of Keggin-type dodecatungstosilicate acid solution was obtained. A mixture of Co(NO<sub>3</sub>)<sub>2</sub>·H<sub>2</sub>O (0.0294 g, 0.1 mmol) and pyridine-2,3-dicarboxylic acid (0.0167 g, 0.1 mmol) was added into the tungstosilicate acid solution. This solution was sealed in a 20 mL Teflon-lined autoclave at 170 °C for 80 h, then the autoclave was cooled to room temperature at 10 °C h<sup>-1</sup>. Rosaline block crystals were filtered and washed with distilled water. Yield: 32.00% (based on W).

### 2.3. X-ray crystallography

A 0.34 × 0.32 × 0.30 mm crystal of the complex was selected for single-crystal X-ray diffraction. The reflection intensities of the crystal were collected at 293 K using a Bruker SMART Apex II CCD area detector single-crystal diffractometer with graphite-monochromated Mo-K $\alpha$  ( $\lambda = 0.71073$  Å) radiation in the range  $\theta = 1.87$ – $24.99^\circ$ . All non-hydrogen atoms were refined with anisotropic displacement parameters. The structure was solved by direct methods and refined by full-matrix least-squares on  $F^2$  using the Shelxtl-97 program package [15]. All hydrogens of the crystal water were added by different Fourier methods while other hydrogens were finally refined as a riding mode using the default Shelxtl parameters.

The detailed crystallographic data and structure refinement parameters are summarized in table 1. Selected bond angles and lengths of the complex are listed in table 2. Crystallographic data for the structures reported in this paper have been deposited in the Cambridge Crystallographic Data Center. CCDC ID of the complex is 999915.

Table 1. Crystal data and structure refinement for the complex.

Parameters	Complex
Formula	(H <sub>3</sub> O) <sub>4</sub> [(CoC <sub>14</sub> H <sub>12</sub> N <sub>2</sub> O <sub>10</sub> ) <sub>1.5</sub> (SiW <sub>12</sub> O <sub>40</sub> )]·2H <sub>2</sub> O
<i>M<sub>r</sub></i>	3625.95
Crystal size (mm <sup>3</sup> )	0.34 × 0.32 × 0.30
Crystal system	Trigonal
Space group	<i>P</i> - <i>3c1</i>
<i>a</i> (Å)	20.363(3)
<i>b</i> (Å)	20.363(3)
<i>c</i> (Å)	27.685(5)
<i>α</i> (°)	90
<i>β</i> (°)	90
<i>γ</i> (°)	120.00
<i>V</i> (Å <sup>3</sup> )	9942(3)
<i>Z</i>	4
<i>D<sub>c</sub></i> /(g cm <sup>-3</sup> )	2.348
Range (°)	1.87–24.99
<i>F</i> (0 0 0), e	5080
<i>hkl</i> range	−24 ≤ <i>h</i> ≤ 24, −24 ≤ <i>k</i> ≤ 24, 19 ≤ <i>l</i> ≤ 32
Refl. measured	70,628
Refl. unique	7346
<i>R</i> <sub>1</sub> [ <i>I</i> > 2σ( <i>I</i> )]	0.0579
<i>R</i> <sub>2</sub> [ <i>I</i> > 2σ( <i>I</i> )]	0.1645
<i>R</i> <sub>int</sub>	0.0383
Parameters	284
GOOF(S)	1.083

Table 2. Selected bond lengths (Å) and angles (°) for the complex with estimated standard deviations in parentheses.

Si(1)–O(10)	1.661(15)	Si(1)–O(19)	1.618(9)
Si(1)–O(19)a	1.618(11)	Si(1)–O(19)b	1.618(11)
W(2)–O(2)	1.9065	W(2)–O(4)	1.7063
W(2)–O(5)	1.9094	W(2)–O(6)	1.9591
W(3)–O(3)	1.9170	W(3)–O(6)	1.9055
W(3)–O(7)	1.7225	W(3)–O(8)	1.8860
Co(1)–O(14)	2.22(2)	Co(1)–O(15)	1.831(17)
Co(1)–N(1)	1.930(17)	Co(1)–O(14)c	2.22(2)
N(1)–C(3)	1.32(3)	C(1)–C(2)	1.27(3)
C(4)–C(5)	1.45(3)	C(4)–C(11)	1.36(3)
O(14)–H(14A)	0.96	C(1)–H(1)	0.93
O(10)–Si(1)–O(19)	109.4(3)	O(10)–Si(1)–O(19)a	109.4(4)
O(2)–W(2)–O(4)	100.39	O(2)–W(2)–O(5)	158.21
O(2)–W(2)–O(8)a	89.35	O(4)–W(2)–O(5)	101.39
O(4)–W(2)–O(6)	99.81	O(4)–W(2)–O(19)	171.17
O(6)–W(2)–O(19)	73.34	O(6)–W(2)–O(8)a	157.45
O(19)–(2)–O(8)a	84.38	O(3)–W(3)–O(6)	89.28
O(7)–W(3)–O(8)	101.75	O(7)–W(3)–O(9)	101.54
O(14)–Co(1)–O(15)	98.8(8)	O(14)–Co(1)–N(1)	93.7(8)
O(15)–Co(1)–N(1)	83.0(7)	N(1)–Co(1)–N(1)c	169.3(6)
O(14)–Co(1)–O(14)c	71.7(8)	O(15)–Co(1)–O(15)c	90.9(8)
Co(1)–O(15)–C(5)	118.8(17)	Co(1)–N(1)–C(3)	127.9(13)
C(2)–C(1)–C(11)	115(2)	C(1)–C(2)–C(3)	124(2)
N(1)–C(4)–C(11)	118(2)	C(5)–C(4)–C(11)	128(2)
O(15)–C(5)–C(4)	113(2)	C(1)–C(11)–C(4)	119(2)
Co(1)–O(14)–H(14A)	109	H(14A)–O(14)–H(14B)	109
C(11)–C(1)–H(1)	122	N(1)–C(3)–H(3)	118

## 2.4. Catalytic reaction

Catalytic reactions were carried out in a continuous-flow fixed-bed microreactor. The catalytic properties of the complex were tested by eliminating methanol. 0.2 ethanol. 0.2c properties of the complex were reaction tube ( $\phi/8$  mm; L/200 mm) as catalyst. A simulacrum of polluted air containing reaction substrate was prepared by bubbling clean air into a bottle filled with methanol solution and diluting the methanol gas with clean and dry air. The initial concentration of reaction substrate was adjusted by adjusting the flow velocity of the bubbling gas and dilution air. The feed gas flowed through the reactor, and the catalytic elimination reaction was carried out at different temperatures, controlled by a thermostat. The concentration of feed gas was detected online by gas chromatographic (GC102-N, FID detector) about every 10 min until the concentration was constant, which means the reaction reaches balance. The inorganic products of the effluent gasses were monitored by a PdCl<sub>2</sub> [0.2 (wt.%) solution and saturated lime-water solution. The concentration of organic compounds of the effluent gasses was analyzed online by a gas GC. Blank experiments were carried out without the complex.

In this research, the elimination rate of methanol was adopted to evaluate the catalytic activity of the catalysts.

## 3. Results and discussion

### 3.1. Crystal structure of the complex

Single-crystal X-ray diffraction analysis reveals that the complex consists of one [SiW<sub>12</sub>O<sub>40</sub>]<sup>4-</sup>, 1.5 [(H<sub>2</sub>O)<sub>2</sub>Co(2,3-pyridine dicarboxylic acid)<sub>2</sub>], four H<sub>3</sub>O<sup>+</sup>, and two water molecules (figure 1). The heteropolyanion [SiW<sub>12</sub>O<sub>40</sub>]<sup>4-</sup> possesses the classical  $\alpha$ -Keggin-type structure with Td symmetry. The Si is surrounded by four oxygens with Si–O bonds ranging from 1.618 to 1.661 Å. The O–Si–O bond angles are 109.4–109.6°, which suggests a distorted tetrahedron formation. All W ions have WO<sub>6</sub> octahedral environments. The W–O bond distances are divided into three groups: W–O<sub>a</sub> (center oxygen atom), 1.9180–2.3532 Å; W–O<sub>b/c</sub> (bridging oxygen), 1.9065–1.9170 Å; W–O<sub>d</sub> (terminal oxygen), 1.7063–1.7225 Å. O–W–O bond angles are between 73.34 and 171.49° which suggests that the WO<sub>6</sub> octahedra are distorted.

The [(H<sub>2</sub>O)<sub>2</sub>Co(2,3-pyridine dicarboxylic acid)<sub>2</sub>] unit has one Co<sup>2+</sup> with two 2,3-pyridine dicarboxylic acids and two water molecules.

The Co(II) has octahedral coordination, bound to two waters, two pairs of N in pyridine and carboxylate oxygen individually from *b*- and *a*-PDCA. Each N and carboxylate oxygen of 2,3-pyridine dicarboxylic acid forms a five-membered ring with Co. Two N, one carboxylate oxygen, and one water constituted the equatorial plane. The other carboxylate oxygen and water occupy the two axial positions [16]. The Co–O distances range from 1.831(17) to 2.22(2) Å and Co–N are 1.930(17) Å, which is similar to the distances of other 2,3-pdc and Co complexes [17, 18]. The unit cell consists of four crystallographically independent molecules (figure 2).

Intramolecular  $\pi$ – $\pi$  stacking exists in the complex (figure 3). The centroid distance of the two aromatic rings (that containing N1 and N1') is 3.5603 Å. The dihedral angle between two aromatic ring planes (N1 and N1') is 11.8° in offset face-to-face  $\pi$ – $\pi$  stacking. The complex exhibits an extended two-dimensional supramolecular network via  $\pi$ – $\pi$  stacking interactions (figure 4).

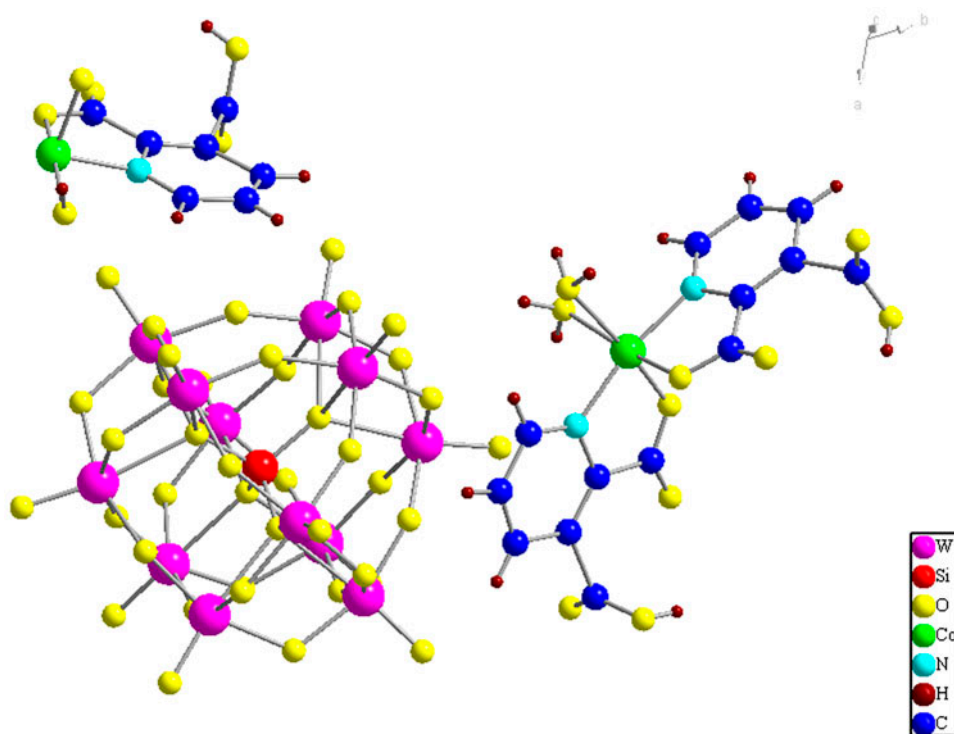


Figure 1. Crystal structure of the complex.

### 3.2. IR spectrum

The IR spectra of  $\text{H}_4\text{SiW}_{12}\text{O}_{40}$  and our complex are shown in figures 5 and 6. The IR of the complex exhibit four characteristic peaks of the Keggin anions from 700 to 1200  $\text{cm}^{-1}$ . Bands at 1130, 983, 922, and 794  $\text{cm}^{-1}$  correspond to  $\nu(\text{Si}-\text{O}_a)$ ,  $\nu(\text{W}-\text{O}_d)$ ,  $\nu(\text{W}-\text{O}_c)$ , and  $\nu(\text{W}-\text{O}_b)$ , respectively [19–21].

A pattern of bands at 3446 and 3099  $\text{cm}^{-1}$  are ascribed (figure 6) to the  $\nu(\text{O}-\text{H})$  in crystallographic water and  $\nu(\text{N}-\text{H})$  of the 2,3-pyridine dicarboxylic acid. 3000, 1602, 1578, and 1441  $\text{cm}^{-1}$  are characteristic peaks of 2,3-pyridine dicarboxylic acid. The absorption at 879  $\text{cm}^{-1}$  is ascribed to H-pyridine ring plane bending vibration; 1725, 1228, and 882  $\text{cm}^{-1}$  are from C=O, C–O and O–H stretches of the  $\text{COO}^-$  groups.

Comparing with  $\text{H}_4\text{SiW}_{12}\text{O}_{40}$ , the four characteristic peaks have a small red-shift or blue-shift, suggesting that 2,3-pyridine dicarboxylic acid interacts with heteropolyacid anion changing the force constants of  $\text{Si}-\text{O}_a$ ,  $\text{W}-\text{O}_d$ , and  $\text{W}-\text{O}_{b/c}$ . The results validate the Keggin framework still remains in the complex.

### 3.3. TG analysis

TG-DTA analysis of the compound was performed from room temperature to 800  $^{\circ}\text{C}$  with 10  $^{\circ}\text{C min}^{-1}$  heating rate in air (figure 7). There are four weight loss steps in the TG-DTA curve. The first occurs from room temperature to 180  $^{\circ}\text{C}$ . The second step shows a 17.46%

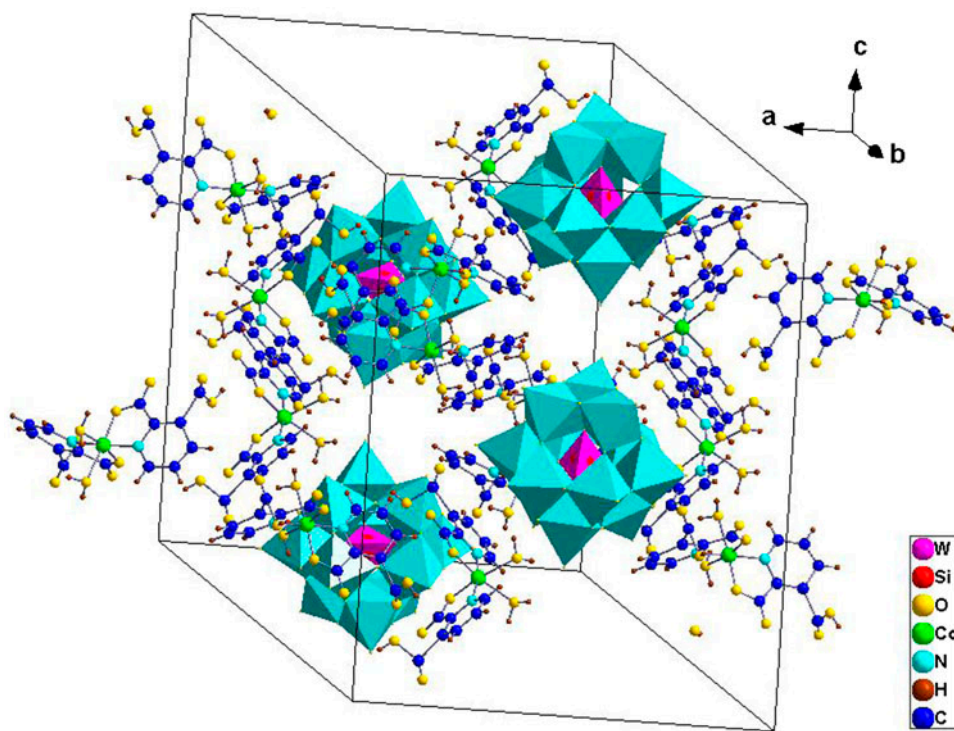


Figure 2. The cell structure of the complex.

weight loss between 280 and 350 °C. From 350 to 530 °C is the third step and the fourth is from 530 to 640 °C with a sharp exothermic peak. The weight losses correspond to removal of crystal water, coordinated water, 2,3-pyridine dicarboxylic acid, and decomposition of silicotungstic heteropolyacid framework, sequentially. The final golden yellow residue may be mixture of  $\text{SiO}_3$ ,  $\text{MoO}_3$ , and  $\text{CoO}$ . The whole process shows an overall 21.53% weight loss which agrees with the calculated value of 23.13%. The complex has a high decomposition temperature to indicate that it has high thermal stability. The results provide basis to set the catalytic reaction temperature.

### 3.4. UV spectrum

The UV spectra of  $\text{H}_4\text{SiW}_{12}\text{O}_{40}$ , 2,3-pyridine dicarboxylic acid, and the complex were measured in aqueous solution at room temperature from 200 to 450 nm (figure 8). The spectrum of  $\text{H}_4\text{SiW}_{12}\text{O}_{40}$  shows two absorptions at 213 and 260 nm, which are the character peaks of heteropolyacid. The peak at 213 nm corresponds with  $\text{O}_d \rightarrow \text{W}$  charge transfer transition of  $\text{W}=\text{O}_d$  bonds. The  $\text{O}_d \rightarrow \text{W}$  charge transfer transitions avoid the influence from the skeletal structure of heteropolyanions. The peak at 260 nm corresponds with  $\text{O}_{b/c} \rightarrow \text{W}$  charge transfer transition of  $\text{W}-\text{O}-\text{W}$  bonds. The 2,3-pyridine dicarboxylic acid absorptions are at 205 and 280 nm, corresponding with the  $\pi-\pi^*$  transitions.

The complex has three absorptions at 209, 257, and 339 nm. The peaks at 209 and 257 nm correspond with  $\text{O}_d \rightarrow \text{W}$  and  $\text{O}_{b/c} \rightarrow \text{W}$  charge transfer transitions, respectively,



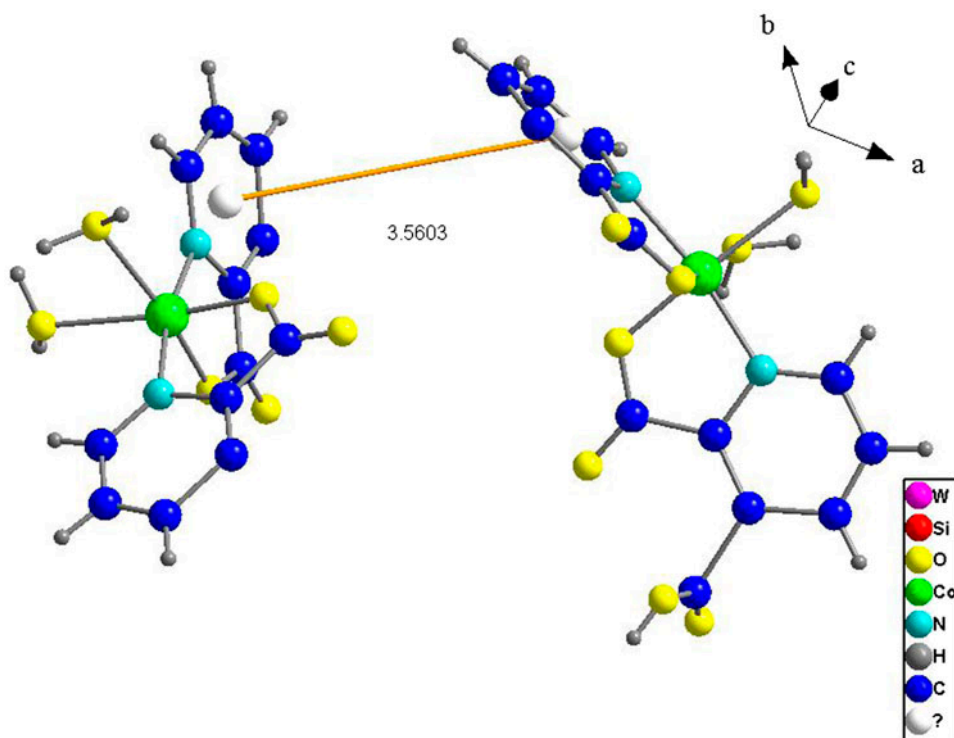


Figure 3. The  $\pi$ - $\pi$  stacking of the complex.

consistent with the skeletal structure of heteropolyanions. According to crystal field theory and semiconductors bond theory, the peak at 339 nm belongs to the absorption of  $\text{Co(II)} \rightarrow \text{O}$  MLCT between 2,3-pyridine dicarboxylic acid and cobalt [22, 23].

### 3.5. Fluorescence properties

$\text{H}_4\text{SiW}_{12}\text{O}_{40}$  and the complex exhibit blue fluorescence [24, 25] (figure 9) at ambient temperature. The maximum emission peaks of  $\text{H}_4\text{SiW}_{12}\text{O}_{40}$  and the complex are located at 471 and 476 nm upon excitation at 236 nm. The fluorescence intensity of  $\text{H}_4\text{SiW}_{12}\text{O}_{40}$  is stronger than of the complex. Fluorescence emission wavelength of the complex is red shifted 5 nm from  $\text{H}_4\text{SiW}_{12}\text{O}_{40}$  [26].

The crystal size of the complex is bigger than  $\text{H}_4\text{SiW}_{12}\text{O}_{40}$ . The electrons have been tied with the polyanion surface, increasing the non-radiative transitions, so that the fluorescence intensity of the complex is lower than  $\text{H}_4\text{SiW}_{12}\text{O}_{40}$ . The silicotungstate anion structure is stabilized when  $[\text{SiW}_{12}\text{O}_{40}]^{4-}$  coordinates with 2,3-pyridine dicarboxylic acid and  $\text{Co}^{2+}$ , reducing the electronic transition energy, causing the red shift.

### 3.6. Cyclic voltammetry

Platinum electrodes were used as the working electrode and the indicator electrode and a calomel electrode as the reference electrode. Scanning voltage is from  $-0.6$  to  $0.6$  V and

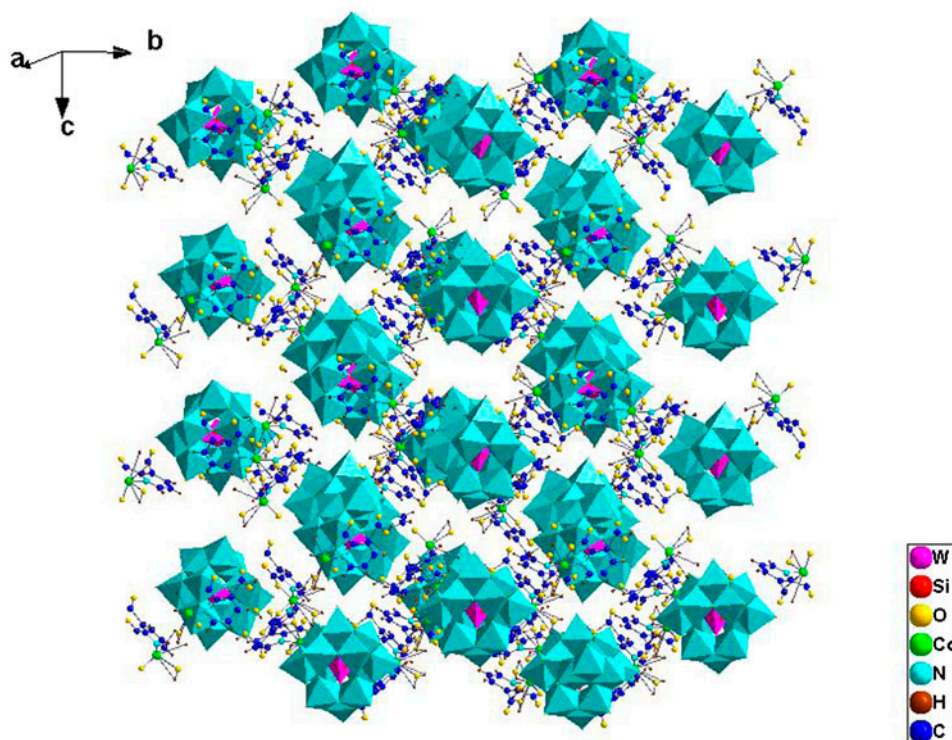


Figure 4. The two-dimensional structure by  $\pi$ - $\pi$  interactions.

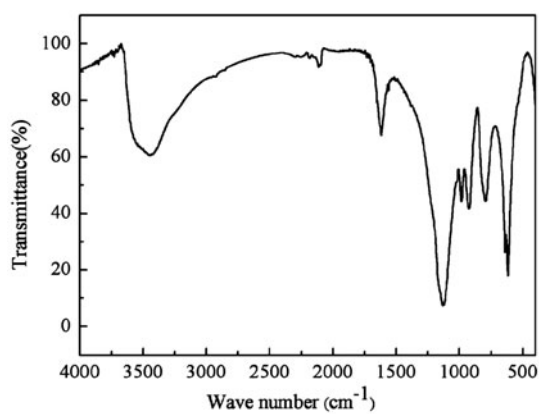


Figure 5. IR spectra of  $\text{H}_4\text{SiW}_{12}\text{O}_{40}$ .

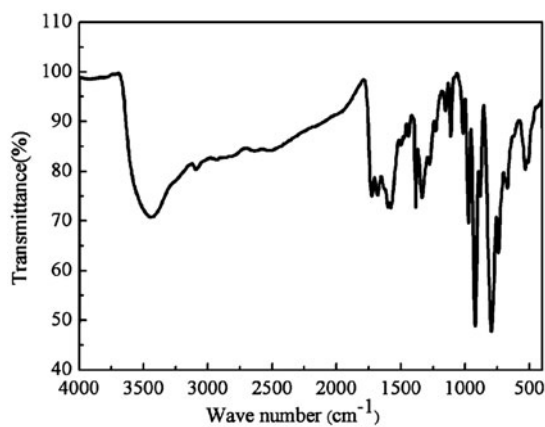


Figure 6. IR spectra of the complex.

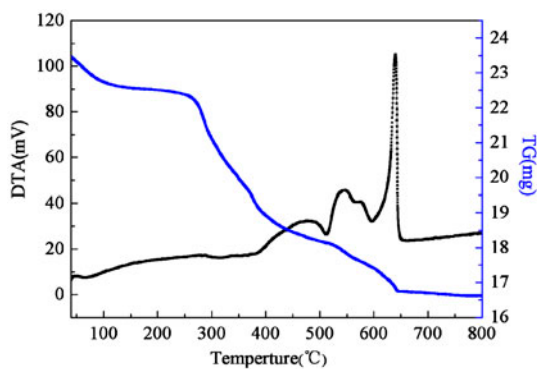


Figure 7. DTA and TG diagrams of the complex.

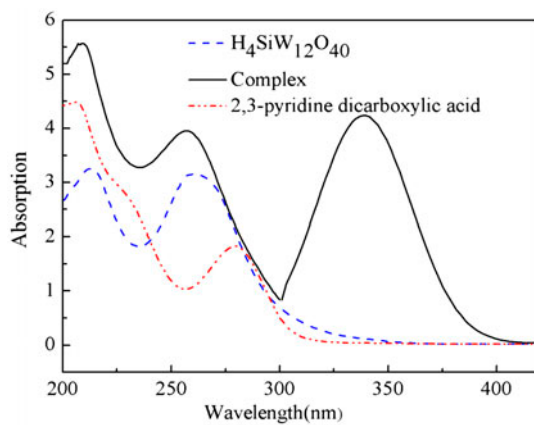


Figure 8. UV spectroscopy of the complex.

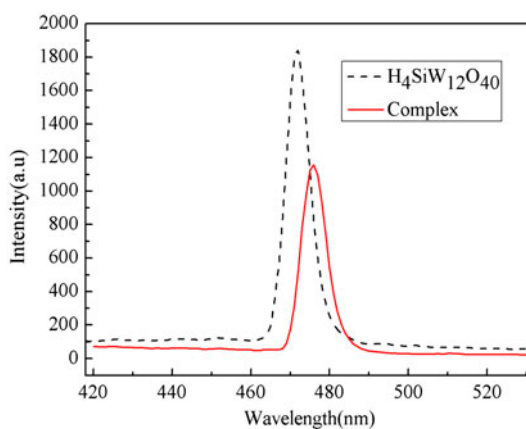
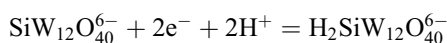
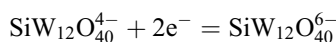


Figure 9. Fluorescence spectra of the complex.

scanning speed is  $10 \text{ mV s}^{-1}$  with  $0.50 \text{ mol L}^{-1}$  NaCl solution as electrolyte. The CV of  $1 \times 10^{-3} \text{ mol L}^{-1}$  complex or  $\text{H}_4\text{SiW}_{12}\text{O}_{40}$  solutions was measured at room temperature using  $\text{N}_2$  to expel dissolved oxygen.

The CV curve (figure 10) shows typical CV behavior. In the potential range from  $-0.6$  to  $+0.1 \text{ V}$ , there is one pair of redox peaks at  $-0.297/-0.489 \text{ V}$  for complex ( $-0.332/-0.280 \text{ V}$  for  $\text{H}_4\text{SiW}_{12}\text{O}_{40}$ ). The redox peaks correspond to two-electron quasi-reversible processes [27–29] of silicotungstate anion, as follows:



The mean peak potentials  $E_{1/2} = ((E_{\text{pa}} + E_{\text{pc}})/2)$  are  $-0.384 \text{ V}$  for complex and  $-0.411 \text{ V}$  for  $\text{H}_4\text{SiW}_{12}\text{O}_{40}$ . According to the literature [30], after the oxidation reaction, if  $E_{1/2} < -0.35 \text{ V}$ ,

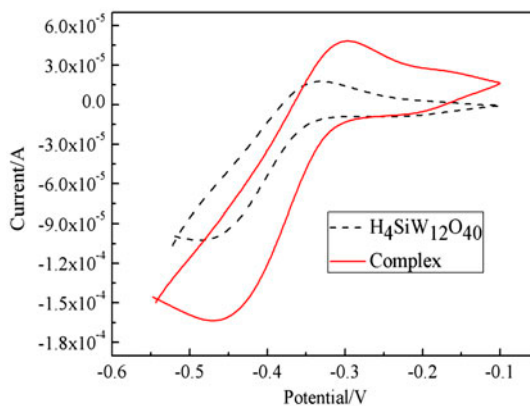


Figure 10. CV curves of  $\text{H}_4\text{SiW}_{12}\text{O}_{40}$  and the complex.

the reductive product heteropoly blues (HPBs) has strong reducing ability. The HPBs can be easily oxidized by  $O_2$  in air to achieve regeneration of the catalyst. Compared with silicotungstate, the onset oxidation potential of the complex is more positive, which means the oxidative capacity has increased. This is propitious to carry on the catalytic oxidation reaction.

### 3.7. Catalytic performance

Blank experiments showed that methanol was hardly eliminated without the complex as the catalyst. There is no new peak except that of methanol in gas GC spectra when the catalytic reaction was undergoing. At the same time, the saturated limewater grew turbid and the color of 0.2%  $PdCl_2$  solution did not change, indicating that  $CO_2$  but not  $CO$  is the product of catalytic elimination of methanol. The controlled trial was done with silicotungstic acid as the catalyst.

When the reaction temperatures were from 30 to 210 °C, catalytic elimination of methanol was tested at an initial methanol concentration of  $2.76 \text{ g m}^{-3}$  and a flow velocity of  $10 \text{ mL min}^{-1}$  over 0.2 g complex or silicotungstate, respectively. Effect of the reaction temperature on the elimination rate of methanol is shown in figure 11. With increase of temperature, the elimination rate increases initially and then falls. When the temperature is 30 °C, the elimination rate of methanol is 36.0% over the silicotungstic acid and 38.7% over compound.

Below 110 °C, the effect of complex and silicotungstic acid are nearly the same. But the elimination effect of the complex is much better than of silicotungstic acid when the temperature is higher than 110 °C. The maximum elimination rate of methanol over complex is 82.6% at 140 °C with the amount eliminated per unit time of  $22.79 \times 10^{-6} \text{ g min}^{-1}$ . The elimination rate of methanol only slightly declines when the temperature continues to rise above 180 °C. Elimination rate of methanol over  $H_4SiW_{12}O_{40}$  declined when the temperature was more than 140 °C and a new peak has been detected by gas chromatographic, indicating that the methanol was not thoroughly mineralized and a by-product formed.

Principally, either for silicotungstate or complex, the heteroatom Si and polyatom W are the highest valence. Heteropolyacids have higher oxidizability than the familiar inorganic

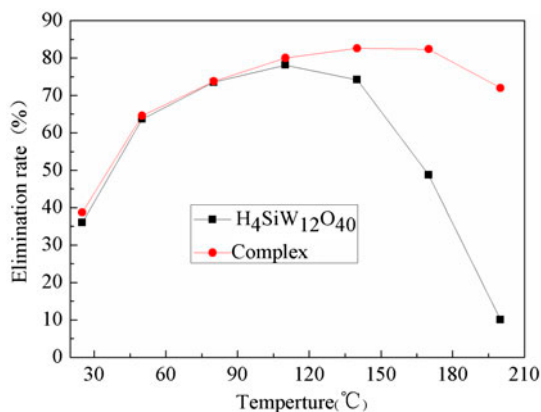


Figure 11. Catalytic performance.

acid and have a cage structure. The special structure creates gaps that allow the small organic molecule into the heteropolyacids' framework. It is called "false liquid," which has the characteristics of homogeneous catalysis. Therefore, both the silicotungstate and complex have the same catalytic abilities to eliminate methanol at low temperature. When the temperature rises to 120 °C, the methanol absorption over silicotungstic acid is reduced, leading to catalytic ability rapidly declining. After 2,3-pyridine dicarboxylic acid coordinates with  $\text{H}_4\text{SiW}_{12}\text{O}_{40}$ , the absorption ability of complex for methanol is improved, enhancing the catalytic reaction. Thus, the elimination rate of the complex still is good at high temperature. The complex has a supramolecular network framework that stabilizes its structure, retaining high catalytic activity at 180 °C, coinciding with its thermostability.

#### 4. Conclusion

This paper describes a Keggin-type organic–inorganic hybrid,  $(\text{H}_3\text{O})_4[(\text{CoC}_{14}\text{H}_{12}\text{N}_2\text{O}_{10})_{1.5}(\text{SiW}_{12}\text{O}_{40})]\cdot 2\text{H}_2\text{O}$ , based on POM, 2,3-pyridine dicarboxylic acid and cobalt nitrate. Single-crystal X-ray diffraction analysis reveals that the complex consists of one  $[\text{SiW}_{12}\text{O}_{40}]^{4-}$ , 1.5 six-coordinate Co with 2,3-pyridine dicarboxylic acid as  $[(\text{H}_2\text{O})_2\text{Co}(2,3\text{-pyridine dicarboxylic acid})_2]$ , four protonated  $\text{H}_3\text{O}^+$ , and two water molecules. The complex exhibits blue fluorescence and has strong oxidation capacity. Compared with  $\text{H}_4\text{SiW}_{12}\text{O}_{40}$  the catalytic ability and stability of the complex are obviously improved. The complex has good catalytic activity from 120 to 180 °C. The elimination of methanol reaches maximum value (82.6%) with the concentration of methanol of  $2.76 \text{ g m}^{-3}$  and the flow velocity  $10 \text{ mL min}^{-1}$  at 140 °C. It can completely convert methanol to  $\text{CO}_2$  and  $\text{H}_2\text{O}$ . This suggests that the complex has strong oxidation ability and good catalytic activity.

Three complexes with Co, Cu, Ag metal, 2,6-pyridine dicarboxylic acid, and tungstosilicate have been described [3]. Their synthesis conditions and reaction products are different, using 2,6-pdc instead of 2,3-pdc. The pyridine-2,6-dicarboxylate decomposes in the synthesis of these compounds, with carboxyl removed from the 6-position of pyridine. The O on the 2-position of pyridine and the N of pyridine coordinated with Co, forming a six-coordinate structure. One Co can coordinate three pyridine molecules. The three pyridine rings perpendicular to each other formed a large volume ligand structure, which cannot form  $\pi$ – $\pi$  stacking. The molecules combine each other only with hydrogen bonds. My complex can form hydrogen bonds and  $\pi$ – $\pi$  stacking, forming a more stable three-dimensional network structure. In addition, my complex has an excellent catalytic activity of eliminating volatile organic compounds, such as methanol.

#### Disclosure statement

No potential conflict of interest was reported by the authors.

#### Funding

This work was supported by Special and Key Laboratory of Functional Materials and Resource Chemistry of Guizhou Provincial Education Department [grant number GAFMRC201302]; Key Laboratory of Theoretical Organic Chemistry and Functional Molecules of Ministry of Education.

## References

- [1] J.-Q. Sha, J. Peng, H.-S. Liu, J. Chen, A. Tian, P.-P. Zhang. *Inorg. Chem.*, **46**, 11183 (2007).
- [2] J.-P. Wang, Q. Wu, J.-Y. Niu. *Sci. China, Ser. B Chem.*, **32**, 210 (2002).
- [3] X.-Y. Liu, H.-L. Nie, L. Wang, R.-D. Huang. *J. Coord. Chem.*, **66**, 444 (2013).
- [4] L. Yang, L.-L. Hou, P.-T. Ma, J.-Y. Niu. *J. Coord. Chem.*, **66**, 1330 (2013).
- [5] S.-H. Yang, X.-Q. Dong, Y.-P. Zhang, H.-M. Hu, G.-L. Xue. *J. Coord. Chem.*, **66**, 1529 (2013).
- [6] L. San Felices, P. Vitoria, J.M. Gutiérrez-Zorrilla, L. Lezama, S. Reinoso. *Inorg. Chem.*, **45**, 7748 (2006).
- [7] A. Harriman, K.J. Elliott, M.A.H. Alamiry, L. Pleux, M. Séverac, Y. Pellegrin, E. Blart, C. Fosse, C. Cannizzo, C.R. Mayer, F. Odobel. *J. Phys. Chem. C*, **113**, 5834 (2009).
- [8] F.-M. Zhang, M.-P. Guo, H.-Q. Ge, J. Wang. *Chem. Ind. Eng. Prog.*, **25**, 1171 (2006).
- [9] H. Liu, Y.-L. Zou, L. Zhang, J.-X. Liu, C.-Y. Song, D.-F. Chai, G.-G. Gao, Y.-F. Qiu. *J. Coord. Chem.*, **67**, 2257 (2014).
- [10] Y. Shen, J. Peng, H.-Q. Zhang, X. Yu, A.M. Bond. *Inorg. Chem.*, **51**, 5146 (2012).
- [11] X.-B. Han, Z.-M. Zhang, T. Zhang, Y.-G. Li, W.-B. Lin, W.-S. You, Z.-M. Su, E.-B. Wang. *J. Am. Chem. Soc.*, **136**, 5359 (2014).
- [12] K. Nomiya, T. Yoshida, Y. Sakai, A. Nanba, S. Tsuruta. *Inorg. Chem.*, **49**, 8247 (2010).
- [13] H. Weiner, H.-J. Lunk, R. Friese, H. Hartl. *Inorg. Chem.*, **44**, 7751 (2005).
- [14] Y. Kikukawa, K. Suzuki, K. Yamaguchi, N. Mizuno. *Inorg. Chem.*, **52**, 8644 (2013).
- [15] G.M. Sheldrick. *SHELXL-97, Program for the Refinement of Crystal Structures [DB]*. University of Göttingen, Germany (1997).
- [16] Q. Jin, J. Zhao, X. Shi. *Chem. J. Chin. Univ.*, **31**, 1496 (2010).
- [17] X. Yan. Synthesis, crystal structure and photo-electric property of a series of Ni-Cd/Zn heterometallic/Ni-Ni homometallic polymers. Dissertation. Liaoning Normal University, p.39 (2013).
- [18] M. Fang. Syntheses and properties of lanthanide (Ln) and Ln-Cu/Co complexes. Dissertation, Nankai University, p.72 (2012).
- [19] K.-L. Xiao, Y.-L. Wang, L.-X. Wu. *Langmuir*, **25**, 6081 (2009).
- [20] L.-B. Yang, Y.-H. Shen, A.-J. Xie, B.-C. Zhang. *J. Phys. Chem. C*, **111**, 5300 (2007).
- [21] Q. Shu, B. Liu, Z.-C. Chao. *Nonferrous. Met. Sci. Eng.*, **4**, 19 (2013).
- [22] Y.-X. Xue. Synthesis, characterization and catalytic performance of modified heteropoly compounds. Dissertation. Jilin University, p.59 (2013).
- [23] D. Li. Phot-electric property of a series of Co-M transition-metal coordination supramolecules (M=Co, Fe, Cd). Dissertation, Liaoning Normal University, p.75 (2012).
- [24] Z.-H. Shi, Y.-S. Zhou, L.-J. Zhang, S.-U. Hassan, N.-N. Qu. *J. Phys. Chem. C*, **118**, 6413 (2014).
- [25] T. Suehiro, N. Hirotsaki, R.-J. Xie. *ACS Appl. Mater. Interfaces*, **3**, 811 (2011).
- [26] W.-N. Wang, W. Widiyastuti, T. Ogi, I.-W. Lenggono, K. Okuyama. *Chem. Mater.*, **19**, 1723 (2007).
- [27] J. Zhang, A.M. Bond. *Inorg. Chem.*, **43**, 8263 (2004).
- [28] J. Zhang, J.-K. Goh, W.-T. Tan, A.M. Bond. *Inorg. Chem.*, **45**, 3732 (2006).
- [29] D. McGregor, B.P. Burton-Pye, I.M. Mbomekalle, P.A. Aparicio, S. Romo, X. López, J.M. Poblet, L.C. Francesconi. *Inorg. Chem.*, **51**, 9017 (2012).
- [30] D.-W. Yu. *Petrochemical Univ.*, **12**, 11 (1999).